

# Impurities, Quantum Interference and Quantum Phase Transitions in $s$ -wave superconductors

Dirk K. Morr and Jaesung Yoon

*Department of Physics, University of Illinois at Chicago, Chicago, IL 60607*

(Dated: March 23, 2022)

We study the effects of quantum interference in impurity structures consisting of two or three magnetic impurities that are located on the surface of an  $s$ -wave superconductor. By using a self-consistent Bogoliubov-de Gennes formalism, we show that quantum interference leads to characteristic signatures not only in the local density of states (LDOS), but also in the spatial form of the superconducting order parameter. We demonstrate that the signatures of quantum interference in the LDOS are qualitatively, and to a large extent quantitatively unaffected by the suppression of the superconducting order parameter near impurities, which illustrates the robustness of quantum interference phenomena. Moreover, we show that by changing the interimpurity distance, or the impurities' scattering strength, the  $s$ -wave superconductor can be tuned through a series of first order quantum phase transitions in which the spin polarization of its ground state changes. In contrast to the single impurity case, this transition is not necessarily accompanied by a  $\pi$ -phase shift of the order parameter, and can in certain cases even lead to its enhancement. Our results demonstrate that the superconductor's LDOS, its spin state, and the spatial form of the superconducting order parameter are determined by a subtle interplay between the relative positions of the impurities and their scattering strength.

PACS numbers: 72.10.-d, 72.10.Fk, 74.25.Jb

## I. INTRODUCTION

Over the last few years, quantum interference effects arising from scattering of conduction electrons by multiple impurities have attracted significant experimental<sup>1,2,3,4,5,6,7</sup> and theoretical<sup>8,9,10,11,12,13,14</sup> attention. For example, Manoharan *et al.*<sup>1</sup> used a corral of magnetic impurities on the surface of a metallic host to demonstrate that quantum interference and the resulting formation of eigenmodes can be used to create quantum images (also called *quantum mirages*). Complementary to this experiment, Derro *et al.*<sup>2</sup>, using scanning tunneling spectroscopy (STS), reported the formation of novel resonance states arising from impurities in the one-dimensional chains of  $\text{YBa}_2\text{Cu}_3\text{O}_{6+x}$ . Quantum interference effects have also been studied in optical quantum corrals<sup>3</sup>, in quantum dots<sup>4</sup>, in triangular corrals<sup>5</sup>, in ferromagnetic islands<sup>6</sup>, and around molecules<sup>7</sup>.

A number of theoretical studies have focused on quantum interference effects in metallic host systems<sup>8</sup>, as well as conventional<sup>9,10,11,12</sup> and unconventional<sup>13,14</sup> superconductors. Superconducting (SC) host systems with  $s$ -wave symmetry are of particular interest for the investigation of quantum interference effects for two reasons. First, a magnetic impurity induces a fermionic bound state in an  $s$ -wave superconductor, which can be used as the object (i.e., the "quantum candle") for the formation of a quantum image<sup>12</sup>, while a non-magnetic impurity does not. This qualitative difference between a magnetic and non-magnetic impurity allows one to study quantum interference effects separately from the formation of fermionic impurity states, in contrast to unconventional superconductors<sup>13,14,15,16</sup>. Second, quantum interference can be used to tune an  $s$ -wave superconductor

through a series of first order quantum phase transition in which the spin polarization of the superconductor's ground state changes<sup>11,15,16,17,18</sup>. Quantum interference phenomena are therefore not only of great fundamental interest, but might also possess important applications in the field of spin electronics<sup>19</sup> and quantum information technology<sup>20</sup>, as these phenomena might lead to the creation of new types of quantum qubits.

In this article, we study quantum interference phenomena arising in structures consisting of two or three magnetic impurities that are located on the surface of an  $s$ -wave superconductor. We employ a self-consistent Bogoliubov-de Gennes (BdG) formalism<sup>21</sup> which allows us to study the effects of quantum interference not only on the formation of impurity bound states, but also on the spatial form of the superconducting order parameter. We obtain three important results. First, we show that quantum interference leads not only to characteristic signatures in the local density of states (LDOS) but also in the spatial form of the superconducting order parameter. In particular, when the distance between impurities is changed, the order parameter at the sites of the impurities (i.e., the *on-site* order parameter) exhibits Friedel-like oscillations. These oscillations mirror the ones in the frequency of the hybridized impurity bound state. Second, we find that the characteristic signatures of quantum interference in the LDOS, such as, e.g., the formation of bonding and antibonding bound states around two magnetic impurities, and the oscillation of the bound state frequencies with interimpurity distance<sup>9,11</sup>, remain qualitatively and to a large extent quantitatively unchanged by the suppression of the order parameter around impurities. This results demonstrate the robustness of quantum interference phenomena. The

physical origin of this robustness lies in the fact that, while the superconducting order parameter is suppressed by impurities, it recovers its bulk value over a length scale which is set by the Fermi wavelength,  $\lambda_F$ , and not by the superconducting coherence length,  $\xi_c$ , where for many  $s$ -wave superconductors typically  $\xi_c \gg \lambda_F$ . Third, we show that quantum interference leads to a series of first order quantum phase transitions, in which the spin polarization of the superconductor's ground state changes. These transitions can be achieved by increasing the impurities' scattering strength, or, which is experimentally more relevant, by changing the interimpurity distance. While this type of quantum phase transition is well understood for a single impurity<sup>17</sup>, we find that the phase transitions associated with multiple impurities exhibit qualitatively new features. In particular, we show that in contrast to the single impurity case, these transitions are not necessarily accompanied by a  $\pi$ -phase shift of the on-site order parameter, and can, in certain cases, even lead to its enhancement. The theoretical predictions for the spatial form of the superconducting order parameter discussed below are of particular importance in light of recent experimental progress in developing Josephson STS<sup>22</sup>, which suggests that our predictions can be tested in the near future.

The rest of the paper is organized as follows. In Sec. II we briefly introduce the BdG formalism. In Secs. III and IV we present our results for the case of a two and three impurity systems, respectively. Finally, in Sec. V we summarize our results and conclusions.

## II. BOGOLIUBOV-DE GENNES FORMALISM

In order to treat quantum interference between electrons that are scattered by multiple impurities and a spatial variation of the superconducting order parameter on equal footing, we use the self-consistent Bogoliubov-de Gennes (BdG) formalism<sup>21</sup>. Within this formalism, one solves the eigenvalue equation

$$\sum_{\mathbf{j}} \begin{pmatrix} H_{\mathbf{ij}}^+ & \Delta_{\mathbf{ij}} \\ \Delta_{\mathbf{ij}}^* & -H_{\mathbf{ij}}^- \end{pmatrix} \begin{pmatrix} u_{\mathbf{j},n} \\ v_{\mathbf{j},n} \end{pmatrix} = E_n \begin{pmatrix} u_{\mathbf{i},n} \\ v_{\mathbf{i},n} \end{pmatrix} \quad (1)$$

with  $H_{\mathbf{ij}}^\pm = t_{\mathbf{ij}} + (\pm J_{\mathbf{i}} S_{\mathbf{i}} - \mu) \delta_{\mathbf{ij}}$ . Here,  $t_{\mathbf{ij}}$  is the hopping integral between sites  $\mathbf{i}$  and  $\mathbf{j}$ , and  $\mu$  is the chemical potential. Below, we consider a two-dimensional system, in which only the nearest-neighbor hopping integral  $t$  and the next-nearest neighbor hopping integral  $t'$  are non-zero. For concreteness, we take  $t'/t = 0.2$  and  $\mu/t = -2$ , leading to an almost circular Fermi surface (FS) with  $k_F \approx \pi/2$ .  $J_{\mathbf{i}}$  and  $S_{\mathbf{i}}$  are the magnetic scattering potential and the spin of the impurity located at site  $\mathbf{i}$ , respectively. Below, we consider for concreteness magnetic impurities with spin  $S = 1/2$ . In an  $s$ -wave superconductor, the superconducting order parameter  $\Delta_{\mathbf{ij}} = \Delta_{\mathbf{i}} \delta_{\mathbf{ij}}$  is

local and given by

$$\Delta_{\mathbf{i}} = -V \sum_n u_{\mathbf{i},n} v_{\mathbf{i},n} \tanh \left( \frac{E_n}{2k_B T} \right), \quad (2)$$

where  $V$  is the effective pairing interaction and the sum runs over all eigenstates of the system. Eqs.(1) and (2) are solved self-consistently in order to obtain the energy,  $E_n$ , of all eigenstates of the system, the local superconducting order parameter,  $\Delta_{\mathbf{i}}$ , as well as the Bogoliubov coefficients  $u_{\mathbf{i},n}, v_{\mathbf{i},n}$  of state  $n$  at site  $\mathbf{i}$ . Below, we take  $V/t = 2.5$ , such that in the clean system, the translationally invariant superconducting order parameter is given by  $\Delta_{\mathbf{i}}/t \approx 0.112$ . Finally, the local density of states at site  $\mathbf{i}$  is obtained via

$$N(\omega, \mathbf{i}) = \sum_n [u_{\mathbf{i},n}^2 \delta(\omega - E_n) + v_{\mathbf{i},n}^2 \delta(\omega + E_n)] \quad (3)$$

Unless otherwise stated, we consider in the following a system with  $N = N_x \times N_y$  sites where  $N_x = 28$  and  $N_y = 18$ . This choice of  $N_x, N_y$  accounts for the spatial anisotropy of the impurity structures considered below.

Note that within the BdG-formalism, one assumes that the impurity spin is a classical, static variable, which corresponds to the limit  $JS = \text{const.}$  and  $S \rightarrow \infty$ . In a fully gaped  $s$ -wave superconductor, this approximation is justified even when considering magnetic impurities with  $S < \infty$ , and in particular small values of  $S$ . Specifically, it was shown<sup>23</sup> that no Kondo effect occurs in a fully gapped  $s$ -wave superconductor for sufficiently small coupling between the magnetic impurities and the delocalized electrons. Hence, it is not necessary to consider the full quantum dynamics of the magnetic impurity, which can thus be treated as a classical, static variable. This finding is also supported by the experimentally measured LDOS around a single magnetic impurity in an  $s$ -wave superconductor<sup>24</sup>. These experiments have reported the existence of two peaks inside the superconducting gap, which are induced by the magnetic impurity. Within the self-consistent BdG-formalism or the non-self-consistent  $\hat{T}$ -matrix approach<sup>15,16,25</sup> these peaks are a direct consequence of the static nature of the magnetic impurity and are the spectroscopic signature of a fermionic (Shiba) bound state.

Finally, within the BdG-formalism, any interaction between the magnetic impurities is only taken into account to the extent that it determines the angle,  $\alpha$ , between the direction of the impurity spins. Within a  $\hat{T}$ -matrix approach, it was shown in Ref.<sup>11</sup> that for two impurities, the cases  $\alpha = 0$  and  $\alpha \neq 0$  are qualitatively very similar<sup>26</sup>. We therefore focus below on the case of impurities with parallel spin, i.e.,  $\alpha = 0$ .

## III. TWO MAGNETIC IMPURITIES

Before considering the effects of two magnetic impurities on the local electronic structure of an  $s$ -wave superconductor, we briefly review the salient features of the

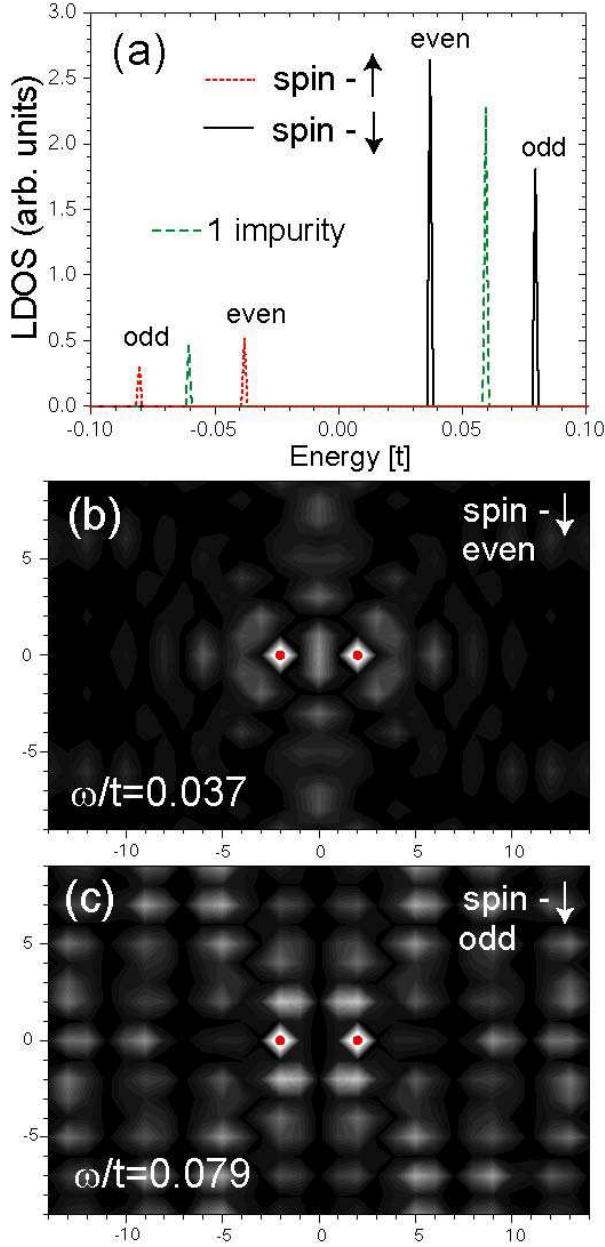


FIG. 1: (Color online). (a) LDOS at  $\mathbf{r}_{1,2}$  as a function of energy for two impurities located at  $\mathbf{r}_{1,2} = (\mp 2, 0)$  (interimpurity distance  $\Delta r = 4$ ) with  $JS/t = 2$  (the lattice constant,  $a_0$ , is set to unity). Spatial intensity plot of the LDOS at (b)  $\omega_{\downarrow}^e/t = 0.037$ , and (c)  $\omega_{\downarrow}^o/t = 0.079$ . The filled red circles denote the positions of the magnetic impurities.

fermionic bound state induced by a single impurity. For a single magnetic impurity with  $\mathbf{S} \parallel \hat{\mathbf{z}}$ , particle-hole mixing in the superconducting state yields a wave-function of the induced bound state that possesses a particle-like and a hole-like component, denoted by  $|p, \uparrow\rangle$  and  $|h, \downarrow\rangle$ , respectively. Here,  $\uparrow, \downarrow$  denote the opposite spin quantum numbers,  $S_z = \pm 1/2$  of the two components. The spectroscopic signature of the bound state are two peaks in the LDOS, as shown in Fig. 1(a). The peak at negative

energies arises from the particle-like component of the wave-function,  $|p, \uparrow\rangle$ , while the peak at positive energies represents the hole-like part,  $|h, \downarrow\rangle$ . These two peaks are therefore also referred to as the spin- $\uparrow$  and spin- $\downarrow$  peaks in the LDOS.

We now turn to the case of two magnetic impurities with parallel spins and  $\mathbf{S} \parallel \hat{\mathbf{z}}$ . If the impurities are infinitely far apart (with interimpurity distance  $\Delta r = \infty$ ), the two bound states with components  $|p, \uparrow, i\rangle$  and  $|h, \downarrow, i\rangle$  ( $i = 1, 2$ ) are degenerate. This degeneracy is lifted for  $\Delta r < \infty$ , since an electron scattered by one of the impurities is in general also scattered by the second impurity, resulting in a coupling of the induced bound states. In order to gain further insight into the nature of this coupling, we consider a toy model in which the unhybridized bound states of energy  $E_0$  are coupled by a hopping term  $D(\Delta r)$ , which depends on the distance,  $\Delta r$ , between the two impurities. This coupling, in turn, leads to the formation of even and odd bound states with energies  $E_{e,o} = E_0 \pm D(\Delta r)$  and a particle-like component of the wavefunction given by  $|p, \uparrow\rangle_{e,o} = (|p, \uparrow, 1\rangle \pm |p, \uparrow, 2\rangle)/\sqrt{2}$ , and similarly for the hole-like component. As a result, the bound state peaks in the LDOS are split [by an energy  $\Delta E = E_e - E_o = 2D(\Delta r)$ ], as shown in Fig. 1(a) for the case of two impurities, located at  $\mathbf{r}_1 = (-2, 0)$  and  $\mathbf{r}_2 = (2, 0)$  ( $\Delta r = 4$ ) with scattering strength  $JS/t = 2$  (in the following, we denote the energies of the spin- $\uparrow$  and spin- $\downarrow$  peaks of the even and odd bound state by  $\omega_{\uparrow,\downarrow}^{e,o}$ , respectively). This splitting of the bound state peaks was also obtained within the non-self-consistent  $\hat{T}$ -matrix formalism<sup>11</sup> (see also Ref.<sup>9</sup>). In Figs. 1(b) and (c) we present a spatial plot of the LDOS at  $\omega_{\downarrow}^e$  and  $\omega_{\downarrow}^o$ , respectively [light (dark) color indicates a large (small) LDOS, and the filled red circles denote the positions of the magnetic impurities]. Fig. 1(c) clearly demonstrates the odd symmetry of the bound state since the LDOS vanishes at any point with equal distance to the two impurities.

In Fig. 2, we present the superconducting order parameter as a function of position for the case of the two impurities considered in Fig. 1. As expected, we find that the order parameter is suppressed in the vicinity of the impurities, with the largest suppression at the impurity sites (indicated by arrows in Fig. 2). Note, however, that the order parameter recovers its bulk value within a few lattice spacing from the impurities. Surprisingly enough, even for the relatively small interimpurity distance of  $\Delta r = 4$  the superconducting order parameter comes close to its bulk value in the region between the two impurities. We therefore conclude that the superconducting order parameter relaxes back to its bulk value on a length scale  $\lambda_r$  of a few lattice spacings. This length-scale  $\lambda_r$  is much shorter than the superconducting coherence length given by  $\xi_c = v_F/\Delta \approx 25a_0$ , where  $v_F$  is the Fermi velocity, and  $a_0$  is the lattice spacing. This result is in agreement with numerical<sup>15</sup> and analytical<sup>27,28</sup> studies of the superconducting order parameter near a single impurity, in which the latter identified  $\lambda_r$  with the

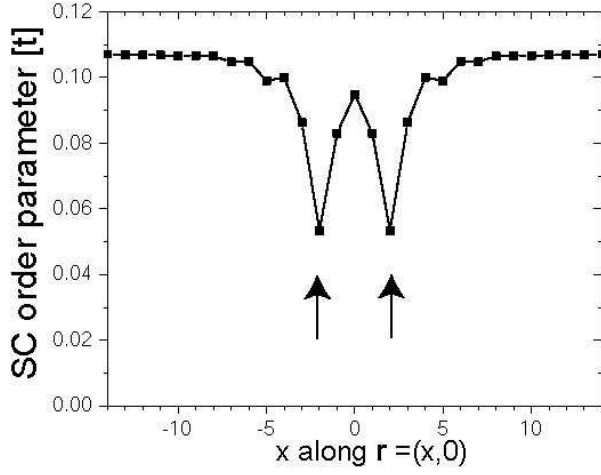


FIG. 2: Superconducting order parameter as a function of position along the line connecting the two impurities at  $\mathbf{r}_{1,2} = (\mp 2, 0)$  considered in Fig. 1. The positions of the impurities are denoted by arrows.

Fermi wavelength  $\lambda_F$ . In our case,  $\lambda_F \approx 4a_0 \ll \xi_c$ .

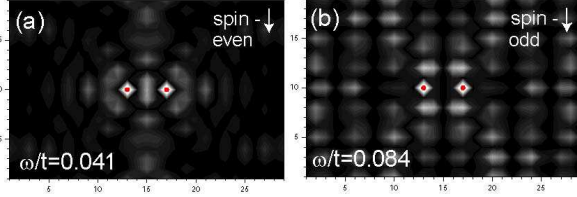


FIG. 3: (Color online). LDOS for a spatially uniform superconducting order parameter. The intensity plot of the LDOS is shown at (a)  $\omega_{\downarrow}^e/t = 0.041$ , and (b)  $\omega_{\downarrow}^o/t = 0.084$ .

In order to ascertain the importance of the order parameter suppression on the frequency and spatial form of the bound states, we computed the LDOS by constraining the superconducting order parameter to its spatially homogeneous bulk value. In this case, the spin- $\uparrow$  and spin- $\downarrow$  peaks of the even and odd bound state are located at  $\omega_{\uparrow}^e/t = -0.042$ ,  $\omega_{\downarrow}^e/t = 0.041$ ,  $\omega_{\uparrow}^o/t = -0.086$  and  $\omega_{\downarrow}^o/t = 0.084$ , respectively. In contrast, when a suppression of the superconducting order parameter is taken into account within the BdG-formalism, the bound state peaks are located at  $\omega_{\uparrow}^e/t = -0.038$ ,  $\omega_{\downarrow}^e/t = 0.037$ ,  $\omega_{\uparrow}^o/t = -0.081$  and  $\omega_{\downarrow}^o/t = 0.079$ , respectively [see Fig. 1(a)]. Thus the spatial suppression of the superconducting order parameter leads to a small shift of the bound state peaks to lower energies (a qualitatively similar effect was observed near a single magnetic impurity, see Ref.<sup>15</sup>). In Figs. 3(a) and (b) we present a spatial intensity plot of the LDOS at  $\omega_{\downarrow}^e/t = 0.041$ , and  $\omega_{\downarrow}^o/t = 0.084$ , respectively. A comparison of Figs. 3(a) and (b) with Figs. 1(b) and (c) immediately shows that the suppression of the superconducting order parameter in the vicinity of the impurities does not lead to percep-

tible changes in the spatial LDOS pattern of the even and odd bound states (for better comparison, the intensity scale for all four figures is the same). Hence, we conclude that characteristic signatures of quantum interference in the LDOS remain qualitatively and to a large extent quantitatively unchanged by the suppression of the order parameter around impurities. This robustness of quantum interference phenomena arises from the fact that the superconducting order parameter recovers its bulk value over a length scale which is typically much shorter than the superconducting coherence length, as discussed above. This conclusion also supports the validity of the results pertaining to two impurity interference effects obtained in Ref.<sup>11</sup> within the non-self-consistent  $\hat{T}$ -matrix approach.

As the distance between the two impurities is changed, the frequency of the even and odd bound state peaks, as well as the splitting between them oscillates<sup>9,11</sup>, as shown in Fig. 4(a). The strength of the coupling,  $D(\Delta r)$ , be-

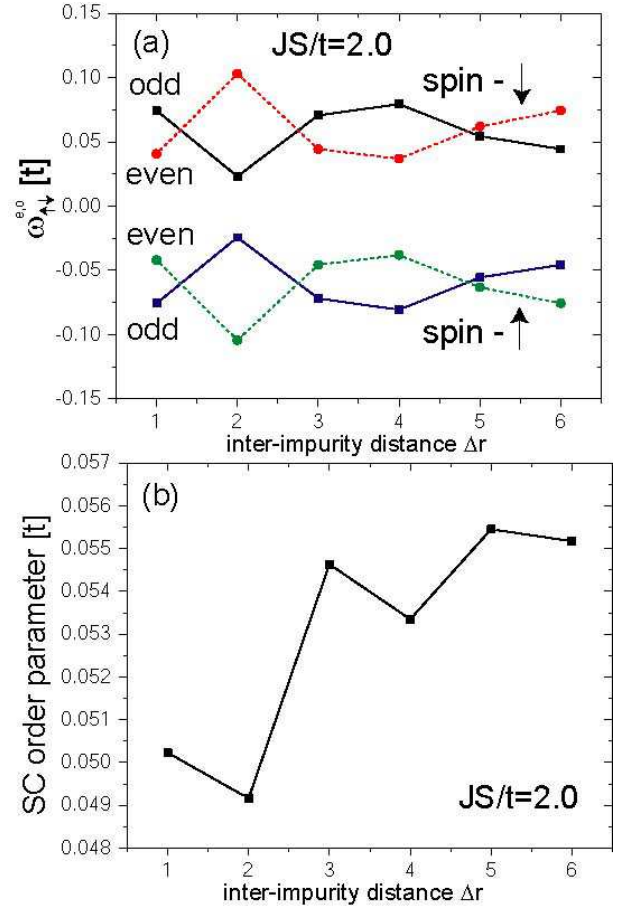


FIG. 4: (Color online). (a) Frequency of the even and odd bound state peaks, and (b) on-site superconducting order parameter (at  $\mathbf{r}_{1,2}$ ) as a function of inter-impurity distance  $\Delta r$  for  $JS/t = 2$ .

tween the impurity states can be directly obtained from the frequency splitting between the even and odd bound states,  $\Delta E = E_e - E_o = 2D(\Delta r)$ . The results shown in

Fig. 4(a) then imply that the effective coupling between the impurity states does not only vary in magnitude, but also changes sign as the distance between the impurities is changed. One obtains, for example,  $D(\Delta r = 2) > 0$ , while  $D(\Delta r = 4) < 0$ . The sign and magnitude of  $D(\Delta r)$  is determined by scattering processes involving both impurities. For example, consider the wave function of an electron that is scattered by the impurity at  $\mathbf{r}_1$ . The sign and magnitude of its wave function at  $\mathbf{r}_2$  (and thus those of the effective coupling) depend (a) on the distance between the impurities due to the  $(k_F r)$ -oscillations of the electronic wave-function, and (b) the scattering phase shift at  $\mathbf{r}_1$ , which is determined by the scattering strength  $JS$ . As a result of the latter, the relative splitting between the even and odd bound states in general varies with  $JS$ , as demonstrated below. Moreover, if the electron's wave function vanishes at  $\mathbf{r}_2$ , the impurity bound states associated with each of the two impurities cannot hybridize and hence remain degenerate<sup>11</sup>.

Complementary to the oscillations of the bound state frequencies, the on-site superconducting order parameter at  $\mathbf{r}_{1,2}$  also oscillates as the distance between the two impurities is increased, as shown in Fig. 4(b). Note that a minimum in the oscillations of the order parameter coincides with a larger splitting between the even and odd bound states. This is expected since a larger splitting implies a stronger coupling between the impurity bound states. At the same time, a larger coupling leads to a stronger effective scattering strength of the two-impurity system, and thus to a larger suppression of the superconducting order parameter.

With increasing scattering strength,  $JS$ , of the two magnetic impurities, the bound states move to lower energies, as follows from a comparison of the LDOS for  $JS/t = 2.0$  [see Fig. 1(a)] with that for  $JS/t = 2.5$  [see Fig. 5(a)], and eventually cross zero energy. For the case of a single magnetic impurity in an  $s$ -wave superconductor, it was first shown by Sakurai<sup>17</sup> that such a zero-energy crossing at a critical value,  $(JS)_{cr}$ , is the signature of a first order quantum phase transition, in which the ground state of the superconductor changes from a state with spin polarization  $\langle S_z \rangle = 0$  to a state with  $\langle S_z \rangle = \pm 1/2$ , depending on the orientation of the magnetic impurity. Here, the spin polarization is defined as

$$\langle S_z \rangle = \frac{1}{2} \int d^2 r \int_{-\infty}^{\infty} d\omega [N_{\uparrow}(\mathbf{r}, \omega) - N_{\downarrow}(\mathbf{r}, \omega)] n_F(\omega), \quad (4)$$

where  $N_{\sigma}(\mathbf{r}, \omega)$  is the LDOS of the electrons with spin  $\sigma = \uparrow, \downarrow$ , and  $n_F$  is the Fermi distribution function. This phase transition arises from a level crossing in the superconductor's free energy,  $\mathcal{F}$ , resulting in a discontinuity of  $\partial \mathcal{F} / \partial J$  at the transition; hence the first order nature of the transition (for a more detailed discussion see Ref.<sup>16</sup>). For a single magnetic impurity, the transition also possesses a characteristic signature in the on-site order parameter which exhibits a discontinuous decrease and changes sign at  $(JS)_{cr}$ , thus undergoing a  $\pi$ -phase

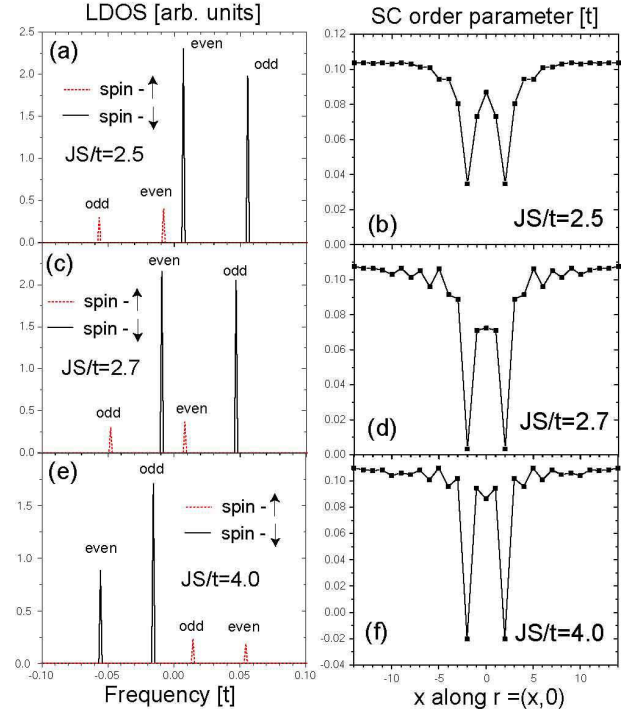


FIG. 5: (Color online). LDOS at  $\mathbf{r}_{1,2}$  as a function of energy (left column) and superconducting order parameter along  $\mathbf{r} = (x, 0)$  (right column) for two impurities located at  $\mathbf{r}_1 = (-2, 0)$  and  $\mathbf{r}_2 = (2, 0)$  for (a),(b)  $JS/t = 2.5$ , (c),(d)  $JS/t = 2.7$ , and (e),(f)  $JS/t = 4.0$ .

shift in comparison to its bulk value.

For the case of two magnetic impurities, quantum interference leads to the emergence of two quantum phase transitions at  $(JS)_{cr,1}$  and  $(JS)_{cr,2}$ , corresponding to the transitions  $\langle S_z \rangle = 0 \rightarrow -1/2$  and  $\langle S_z \rangle = -1/2 \rightarrow -1$ , respectively, of the ground state's spin polarization. Specifically, the even bound state crosses zero energy at  $(JS)_{cr,1}/t \approx 2.54$ , such that for  $JS > (JS)_{cr,1}$ , the spin- $\uparrow$  (spin- $\downarrow$ ) peak of the even bound state is hole-like (particle-like), as shown in Fig. 5(c) for  $JS/t = 2.7$ . However, while in the non-self-consistent  $\hat{T}$ -matrix approach, the frequency of the even bound state,  $\omega_{\uparrow,\downarrow}^e$  evolves continuously as a function of  $JS$  and reaches zero at the transition<sup>11</sup>, within the BdG formalism,  $\omega_{\uparrow,\downarrow}^e$  crosses zero-energy discontinuously at  $(JS)_{cr}$ , similar to the transition associated with a single magnetic impurity<sup>15</sup>. Specifically, for  $(JS)_{cr,1} - 0^+$  one finds  $\omega_{\uparrow,\downarrow}^e/t = \mp 0.005$ , while for  $(JS)_{cr,1} + 0^+$  one has  $\omega_{\uparrow,\downarrow}^e/t = \pm 0.001$  [the upper (lower) sign corresponds to the spin- $\uparrow$  (spin- $\downarrow$ ) peak]. Interestingly enough, we find that the energy of the odd bound state does not exhibit a discontinuity at  $(JS)_{cr,1}$ . A similar discontinuous zero-energy crossing of the bound state energies is found at all phase transitions discussed below. The second quantum phase transition (with  $\langle S_z \rangle = -1/2 \rightarrow -1$ ) occurs at  $(JS)_{cr,2}/t = 3.69$  when the odd bound state crosses zero energy, such that for  $JS > (JS)_{cr,2}$ , all spin- $\uparrow$  (spin- $\downarrow$ ) peaks are now lo-



cated at positive (negative) energies [see Fig. 5(e) for  $JS = 4.0t > (JS)_{cr,2}$ ].

In Figs. 5(b), (d) and (f) we plot the superconducting order parameter as a function of position for the three values of  $JS$  considered above. We find that the two phase transitions are accompanied by discontinuous changes of the on-site superconducting order parameter at  $\mathbf{r}_{1,2}$ , as follows directly from Fig. 6(a) where we plot the on-site order parameter as a function of  $JS$ . Note,

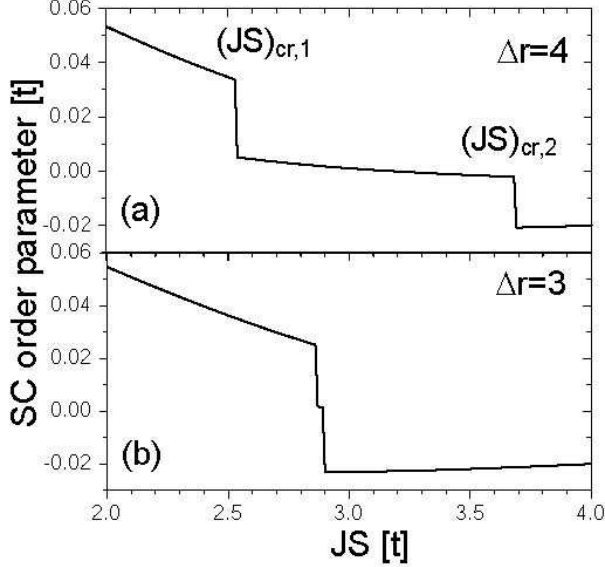


FIG. 6: On-site superconducting order parameter as a function of  $JS$  for two impurities located at (a)  $\mathbf{r}_{1,2} = (\mp 2, 0)$  with  $\Delta r = 4$  (the critical values  $(JS)_{cr,j}$  are indicated by arrows) and (b)  $\mathbf{r}_1 = (-1, 0)$  and  $\mathbf{r}_2 = (2, 0)$  with  $\Delta r = 3$ .

however, that while the on-site order parameter is reduced at  $(JS)_{cr,1}$ , it remains positive and does not exhibit a  $\pi$ -phase shift, in qualitative contrast to the case of a single magnetic impurity<sup>15,16,17</sup>. For  $JS > (JS)_{cr,1}$  the superconducting order parameter decreases continuously with increasing  $JS$ , and crosses zero at  $JS/t \approx 3.15$ . This zero-crossing of the on-site order parameter does not lead to any signature in the LDOS. At  $(JS)_{cr,2}$ , the superconducting order parameter at  $\mathbf{r}_{1,2}$  exhibits a second discontinuity. Note, however, that in contrast to the discontinuous change at  $(JS)_{cr,1}$ , where the magnitude of the superconducting order parameter decreases, its magnitude increases at  $(JS)_{cr,2}$ . Interestingly enough, the suppression of the superconducting order parameter becomes spatially more confined when the system undergoes a phase transition. For example, the superconducting order parameter at  $\mathbf{r}_{nn} = (3, 0)$ , i.e., one site away from one of the impurities, is much less reduced from its bulk value for  $JS > (JS)_{cr,1}$  [Fig. 5(d)] than for  $JS < (JS)_{cr,1}$  [Fig. 5(b)]. Moreover, for  $JS > (JS)_{cr,2}$  the order parameter at  $\mathbf{r}_{nn}$  as well as between the two impurities at  $\mathbf{r} = (0, 0)$  is quite close to its bulk value [see Fig. 5(f)], in contrast to the results shown in Fig. 5(b) for  $JS < (JS)_{cr,1}$ .

For all interimpurity distances we considered, the dependence of the LDOS and the superconducting order parameter on the scattering strength is similar to the one discussed above. However, the splitting between  $(JS)_{cr,1}$  and  $(JS)_{cr,2}$  depends strongly on the interimpurity distance. For example, for  $\Delta r = 3$ , the two phase transitions occur at  $(JS)_{cr,1}/t = 2.87$  and  $(JS)_{cr,2}/t = 2.9$ , as shown in Fig. 6(b). The splitting between the two critical values is thus considerably smaller than for the case  $\Delta r = 4$  shown in Fig. 6(a). We note, however, that while the splitting between the two critical values is small, they are nevertheless reduced from the critical value of a single magnetic impurity given by  $(JS)_{cr}/t = 3.09$ . At the same time, we find that the energy splitting between the odd and even bound states is considerably smaller for  $\Delta r = 3$  than for  $\Delta r = 4$ . In particular, for  $\Delta r = 3$  the frequency splitting between the even and odd bound state peaks at  $(JS)_{cr,1}$  is  $\Delta\omega \approx 0.0056t$ , while for  $\Delta r = 4$  at  $(JS)_{cr,1}$ , the frequency splitting is about one order of magnitude larger with  $\Delta\omega \approx 0.056t$ . We therefore conclude that the splitting of the critical values of  $JS$ , similar to the splitting of the even and odd bound state energies depends on the effective coupling between the two impurities. Hence,  $(JS)_{cr,1,2}$  are functions of  $\Delta r$ . In this regard, it is interesting to note that with increasing  $JS$ , the frequency splitting between the odd and even bound states increases for  $\Delta r = 4$ , but decreases for  $\Delta r = 3$ , as can be seen from a comparison of Fig. 4(a) and Fig. 7(b). This effect directly reflects the dependence of the scattering phase shift on  $JS$ , as discussed above.

In Fig. 7(a) we present the superconducting order parameter at  $\mathbf{r}_{1,2}$  for several values of  $JS$  as a function of inter-impurity distance,  $\Delta r$ . For  $JS/t = 2$ , the order parameter exhibits only weak Friedel-like oscillations when the distance between the impurities is varied (see also Fig. 2). In contrast, for  $JS/t = 2.7$ , the on-site superconducting order parameter,  $\Delta_{\mathbf{r}_{1,2}}$ , oscillates much more strongly when the interimpurity distance is changed, for example, from  $\Delta_{\mathbf{r}_{1,2}} = 0.030t$  at  $\Delta r = 3$  to  $\Delta_{\mathbf{r}_{1,2}} = 0.003t$  at  $\Delta r = 4$ . The reason for this strong variation becomes clear when one considers Fig. 6. For  $\Delta r = 3$ , one finds  $(JS)_{cr,1}/t > JS/t = 2.7$ , implying that the spin polarization of the superconductor is  $\langle S_z \rangle = 0$ . In contrast, for  $\Delta r = 4$  one has  $(JS)_{cr,1}/t < JS/t = 2.7 < (JS)_{cr,2}/t$ , yielding  $\langle S_z \rangle = -1/2$ . In other words, for  $JS/t = 2.7$  the superconductor undergoes a first order phase transition when the interimpurity distance is changed from  $\Delta r = 3$  with spin polarization  $\langle S_z \rangle = 0$  to  $\Delta r = 4$  where  $\langle S_z \rangle = -1/2$ . As a result, the superconducting order parameter varies strongly between  $\Delta r = 3$  and  $\Delta r = 4$ , as shown in Fig. 7(a). This effect directly reflects the dependence of  $(JS)_{cr,1(2)}$  on  $\Delta r$ , as discussed above.

While for  $JS/t = 2.7$ , the spin polarization of the superconductor's ground state changes between  $\langle S_z \rangle = 0$  and  $\langle S_z \rangle = -1/2$ , we find that for  $JS/t = 3.0$ , its spin polarization varies between  $\langle S_z \rangle = -1/2$  [for  $\Delta r = 2, 4, 6$  where  $(JS)_{cr,1}/t < JS/t = 3.0 < (JS)_{cr,2}/t$ ] and  $\langle S_z \rangle = -1$  [for  $\Delta r = 1, 3, 5$  where  $(JS)_{cr,2}/t < JS/t = 3.0$ ].

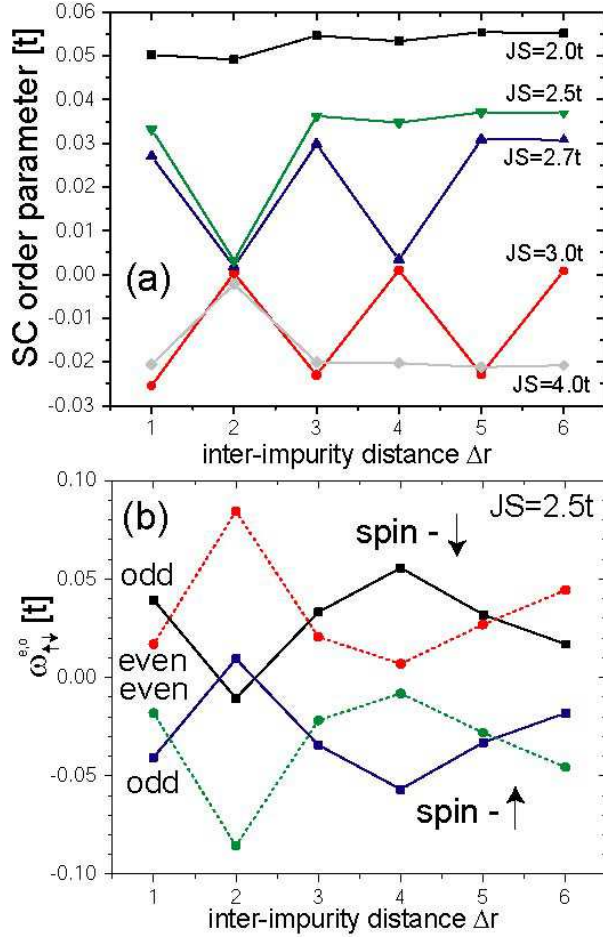


FIG. 7: (Color online). (a) Superconducting order parameter,  $\Delta r_{1,2}$  at  $\mathbf{r}_{1,2}$  as a function of interimpurity distance,  $\Delta r$ , for several values of  $JS/t$ . (b) Frequency of the even and odd bound state peaks as a function of inter-impurity distance  $\Delta r$  for  $JS/t = 2.5$ .

Finally, for  $JS/t = 4.0$ , the behavior of the superconducting order parameter is complementary to that at  $JS/t = 2.5$ , in that the superconductor's spin polarization is  $\langle S_z \rangle = -1/2$  for  $\Delta r = 2$ , and  $\langle S_z \rangle = -1$  for  $\Delta r \neq 2$  (while  $\langle S_z \rangle = 0$  for  $JS/t = 2.5$  and  $\Delta r \neq 2$ ).

In order to explore the interplay between the position of the bound state peaks in the LDOS and the superconducting order parameter further, we plot in Fig. 7(b) the energies of the even and odd bound states as a function of inter-impurity distance for  $JS/t = 2.5$ . For  $\Delta r = 2$ , the spin polarization of the superconductor is given by  $\langle S_z \rangle = -1/2$ , since the odd bound state has crossed zero energy. At the same time, the superconducting order parameter at  $\mathbf{r}_{1,2}$  is significantly reduced [see Fig. 7(a)]. In contrast, for all other interimpurity distances, no zero-energy crossing of the bound state peaks is observed, and the superconducting order parameter at  $\mathbf{r}_{1,2}$  is significantly larger than that for  $\Delta r = 2$ . Both results imply that for  $\Delta r \neq 2$ , one has  $\langle S_z \rangle = 0$ .

#### IV. THREE MAGNETIC IMPURITIES

We next consider the case of three magnetic impurities, for which the superconducting order parameter exhibits an interesting behavior at the first order phase transitions. Specifically, we study three impurities with parallel spins ( $\mathbf{S} \parallel \hat{\mathbf{z}}$ ) that are located at  $\mathbf{r}_{1,3} = (\mp x, 0)$  and  $\mathbf{r}_2 = (0, 0)$ . Quantum interference of scattered electrons again lifts the degeneracy of the fermionic bound states associated with each of the impurities, leading to the emergence of six peaks in the LDOS. In order to gain insight into the symmetry of the hybridized bound states, we assume that the *unhybridized* bound states of energy  $E_0$  are coupled to the nearest neighbor (next nearest neighbor) state via a hopping term  $K$  ( $K'$ ). The resulting energies of the three hybridized bound states are then given by

$$E_{\text{odd}} = E_0 - K'$$

$$E_{\pm} = E_0 + \frac{K'}{2} \pm \sqrt{\frac{(K')^2}{4} + 2K^2}$$

The wavefunction with energy  $E_{\text{odd}}$  is given by  $\Psi_{\text{odd}} = (\psi_1 - \psi_3)/\sqrt{2}$  where  $\psi_i$  is the wavefunction of the unhybridized fermionic bound state induced by the impurity at  $\mathbf{r}_i$ . Note that the wavefunction  $\Psi_{\text{odd}}$  is odd and thus vanishes at any point in space with equal distance to  $\mathbf{r}_1$  and  $\mathbf{r}_3$ . Thus the odd bound state vanishes in particular at  $\mathbf{r}_2$ , which, as discussed below, is important for the behavior of the superconducting order parameter at the first order phase transitions. The wavefunctions with energies  $E_{\pm}$  for the case  $K' = 0$  are given by  $\Psi_{\pm} = \sqrt{2}(\psi_1 \pm \psi_2/\sqrt{2} - \psi_3)/\sqrt{5}$ , respectively (we omit their forms for  $K' \neq 0$  since these are quite cumbersome and irrelevant for the discussion below). Note that the energy of the odd bound state always lies between those of the  $\Psi_{\pm}$ -states, with the energy difference between the  $\Psi_{\pm}$ -states and the  $\Psi_{\text{odd}}$ -state given by

$$\Delta E_{\pm} = E_{\pm} - E_{\text{odd}} = \frac{3K'}{2} \pm \sqrt{\frac{(K')^2}{4} + 2K^2}. \quad (5)$$

Next, we consider the concrete case of three impurities located at  $\mathbf{r}_{1,3} = (\mp 2, 0)$  and  $\mathbf{r}_2 = (0, 0)$  with nearest neighbor distance  $\Delta r = 2$ . The resulting LDOS as a function of frequency at  $\mathbf{r}_{1,3}$  for four different values of  $JS$  is shown in Fig. 8. As discussed above, one finds six peaks in the LDOS, three peaks each arising from the components of the hybridized bound state wave functions with  $S_z = +1/2$  (spin- $\uparrow$  peaks) and  $S_z = -1/2$  (spin- $\downarrow$  peaks). For small  $JS$  [Fig. 8(a)], all spin- $\downarrow$  (spin- $\uparrow$ ) peaks are hole-like (particle-like) and thus located at  $\omega > 0$  ( $\omega < 0$ ). With increasing  $JS$ , the peaks move towards zero energy, and a phase transition occurs when the first bound state crosses zero energy at  $(JS)_{\text{cr},1}/t = 1.98$ . At this first order transition, the spin polarization of the superconductors changes from  $\langle S_z \rangle = 0$  to  $\langle S_z \rangle = -1/2$ . For  $JS = 2.5t > (JS)_{\text{cr},1}$  [see Fig. 8(b)] one of the spin- $\downarrow$  (spin- $\uparrow$ ) peaks is located at negative (positive) energies.

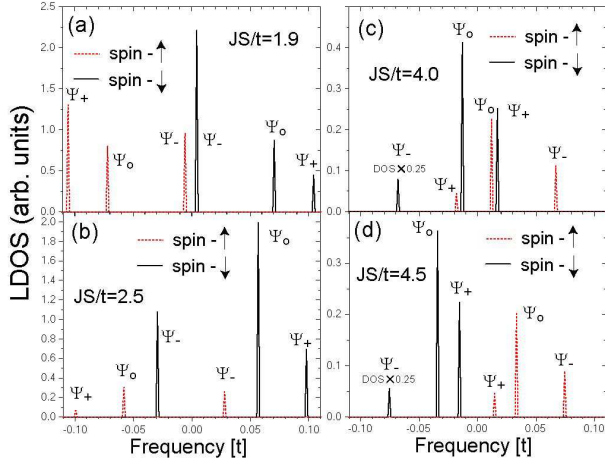


FIG. 8: (Color online). LDOS as a function of frequency at  $\mathbf{r}_{1,3}$  for the case of three impurities with interimpurity distance  $\Delta r = 2$  and four different values of  $JS$ : (a)  $JS/t = 1.9$ , (b)  $JS/t = 2.5$ , (c)  $JS/t = 4.0$ , and (d)  $JS/t = 4.5$ . The results in (a) were obtained for a lattice with  $N_x = 34$  and  $N_y = 22$ , those in (b)-(d) for a lattice with  $N_x = 28$  and  $N_y = 18$  (see Ref.<sup>29</sup>).

The spatial pattern of the three bound states at the frequencies of the spin- $\uparrow$  and spin- $\downarrow$  peaks is shown in Fig. 9. The bound state whose spatial pattern is shown

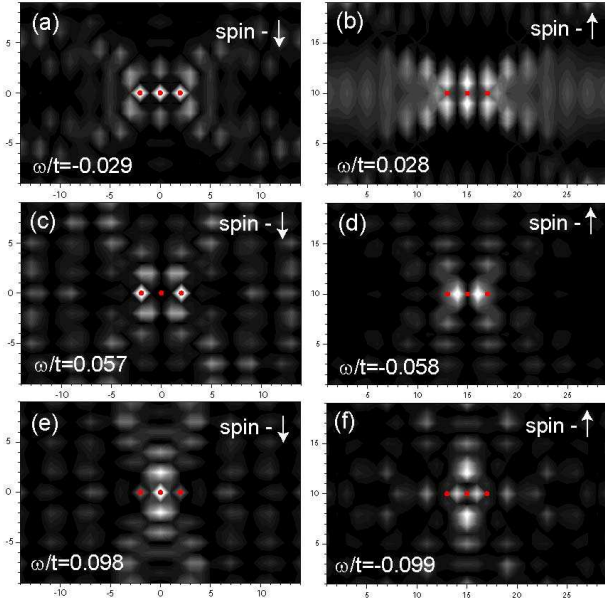


FIG. 9: (Color online). Spatial intensity plot of the LDOS for three impurities with  $JS/t = 2.5$  at the frequency of the spin- $\downarrow$  peaks and spin- $\uparrow$  peaks of the  $\Psi_-$ -state [(a) and (b)], the  $\Psi_{odd}$ -state [(c) and (d)], and the  $\Psi_+$ -state [(e) and (f)], respectively.

in Fig. 9(c) and (d) is easily identified as the odd bound state with wavefunction  $\Psi_{odd}$ . In order to identify the  $\Psi_{\pm}$ -bound states, we use Eq.(5) and the results presented

in Figs. 4(a) and 7(b). Since  $K = D(\Delta r = 2) > 0$ , and  $K' = D(\Delta r = 4) < 0$ , we obtain from Eq.(5) that  $|\Delta E_-| > |\Delta E_+|$ . An inspection of the LDOS in Fig. 8 then allows us to identify the bound state whose spatial pattern is shown in Figs. 9(a) and (b) as the  $\Psi_-$ -state [which crosses zero energy at  $(JS)_{cr,1}$ ], while the bound state shown in Figs. 9(e) and (f) is the  $\Psi_+$ -state. This result is also supported by our analysis of the  $LDOS \sim |\Psi_{\pm}|^2$  based on the value of  $\Psi_{\pm}$  at  $\mathbf{r}_{1,2}$ . Finally, we note that the spatial structure of these bound states remains almost unchanged as  $JS$  is increased and the superconductor undergoes a first order transition.

The zero energy crossing of the  $\Psi_-$ -state at  $(JS)_{cr,1}$  is accompanied by a discontinuous jump in the superconducting order parameter at all three impurity sites, as shown in Fig. 10(a). While the superconducting order

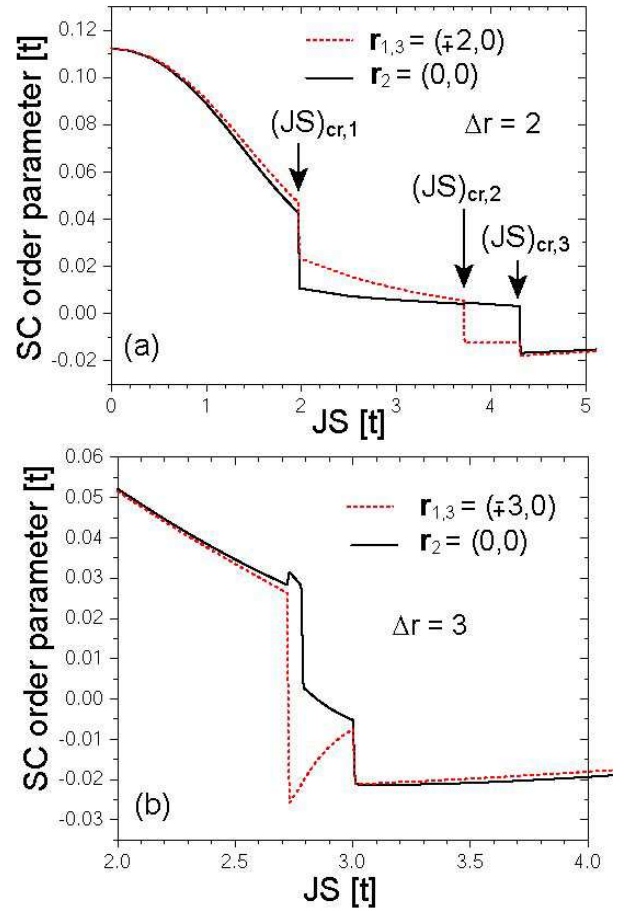


FIG. 10: (Color online). On-site superconducting order parameter at  $\mathbf{r}_{1,2,3}$  as a function of  $JS$  for three impurities with nearest neighbor distance (a)  $\Delta r = 2$  (the critical values  $(JS)_{cr,j}$  are indicated by arrows) and (b)  $\Delta r = 3$ .

parameter is reduced at the transition, it remains positive, and does not undergo a  $\pi$ -phase shift. When  $JS$  is further increased, the odd bound state crosses zero energy at  $(JS)_{cr,2}/t = 3.72$ , and the superconductor undergoes a first order phase transition to a state with  $\langle S_z \rangle = -1$  [a spatial intensity plot of the LDOS at fre-



quency of the odd bound state is shown in Figs. 9(c) and (d)]. For  $JS = 4.0t > (JS)_{cr,2}$ , two spin- $\downarrow$  (spin- $\uparrow$ ) peak are located at  $\omega < 0$  ( $\omega > 0$ ) [see Fig. 8(c)]. Since the odd bound state vanishes at  $\mathbf{r}_2$ , we find that the superconducting order parameter at  $\mathbf{r}_2$  remains unaffected by the zero energy crossing, while that at  $\mathbf{r}_{1,3}$  changes discontinuously and undergoes a  $\pi$ -phase shift, as shown in Fig. 10(a). Finally, at  $(JS)_{cr,3}/t = 4.31$  the  $\Psi_+$ -bound state crosses zero energy, and the superconductor undergoes a first order phase transition to a state with a spin polarization  $\langle S_z \rangle = -3/2$  [the spatial LDOS intensity of the  $\Psi_+$  bound state is shown in Figs. 9(e) and (f)]. All spin- $\downarrow$  (spin- $\uparrow$ ) peaks are now located at  $\omega < 0$  ( $\omega > 0$ ), as shown in Fig. 8(c) for  $JS = 4.5t > (JS)_{cr,3}$ . At  $(JS)_{cr,3}$ , the superconducting order parameter at all three impurity sites again changes discontinuously, and increases in magnitude, as shown in Fig. 10(a). However, only the order parameter at  $\mathbf{r}_2$  changes sign at this transition.

The behavior of the superconducting order parameter at the first order phase transitions is different from the above scenario when the nearest neighbor interimpurity distance is increased to  $\Delta r = 3$  and the impurities are located at  $\mathbf{r}_{1,3} = (\mp 3, 0)$  and  $\mathbf{r}_2 = (0, 0)$ . In this case, the three phase transitions occur in a much smaller range of  $JS$  than for  $\Delta r = 2$ , with  $(JS)_{cr,1}/t = 2.73$ ,  $(JS)_{cr,2}/t = 2.79$  and  $(JS)_{cr,3}/t = 3.01$ . As discussed above, this indicates a weaker coupling between the unhybridized bound states of the impurities, and we therefore also expect a smaller frequency splitting between the peaks of the three bound states in the LDOS. This smaller frequency splitting is directly evident from a comparison of the LDOS for  $\Delta r = 3$  and  $JS/t = 2.78 > (JS)_{cr,1}$  shown in Fig. 11, with the LDOS for  $\Delta r = 2$  shown in Fig. 8. Moreover, the fact that the energy splittings between the peaks,  $|\Delta E_{\pm}|$ , is almost identical, implies that the effect of  $K' = D(\Delta r = 6)$  can be neglected in comparison to that of  $K = D(\Delta r = 3)$ . A more detailed analysis of  $\Psi_{\pm}$  then shows that for  $\Delta r = 3$ , the relative energies of the  $\Psi_+$  and  $\Psi_-$  bound states are reversed in comparison to the case  $\Delta r = 2$ : the peaks of the  $\Psi_-$  bound state are now located at higher energies than those of the  $\Psi_+$  bound state. Thus the  $\Psi_+$  bound state crosses zero energy at  $(JS)_{cr,1}$ , the  $\Psi_{odd}$  bound state at  $(JS)_{cr,2}$ , and the  $\Psi_-$  bound state at  $(JS)_{cr,3}$ . Interestingly enough, the LDOS shown in Fig. 11(a) at  $\mathbf{r}_{1,3}$  only possesses five peaks. The reason for the “missing” peak becomes evident when one considers the spatial form of the LDOS at the bound state frequencies. Specifically, the LDOS of the  $\Psi_+$  bound state at the frequency of the spin- $\uparrow$  peak vanishes at  $\mathbf{r}_{1,3}$ , as shown in Fig. 11(c), which explains the absence of the sixth bound state peak in Fig. 11(a). Note that the LDOS at the spin- $\downarrow$  peak of the  $\Psi_+$  bound state does not vanish at  $\mathbf{r}_{1,3}$  [see Fig. 11(b)]. This spatial form of the  $\Psi_+$  bound state possesses an interesting consequence for the behavior of the superconducting order parameter at  $(JS)_{cr,1}$ , as shown in Fig. 10(b). Specifically, at  $(JS)_{cr,1}$  the superconducting order parameter at  $\mathbf{r}_2$  is reduced, while the order parameter at  $\mathbf{r}_{1,3}$  is

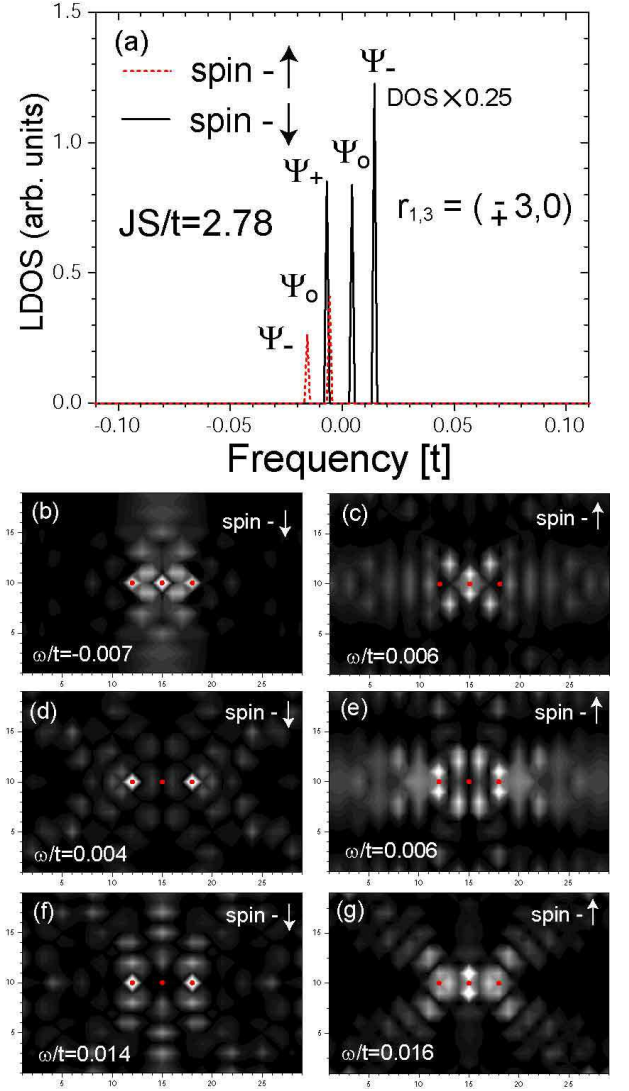


FIG. 11: (Color online). LDOS for three impurities with  $\Delta r = 3$  and  $JS/t = 2.78 > (JS)_{cr,1}$ . (a) LDOS at  $\mathbf{r}_{1,3}$  as a function of frequency. Spatial intensity plot of the LDOS at the frequency of the spin- $\downarrow$  peaks and spin- $\uparrow$  peaks of the  $\Psi_+$ -state [(b) and (c)], the  $\Psi_{odd}$ -state [(d) and (e)], and the  $\Psi_-$ -state [(f) and (g)], respectively.

slightly enhanced. This behavior of the superconducting order parameter is quite different from that at  $(JS)_{cr,3}$ , when the  $\Psi_-$  bound state crosses zero energy. Since neither the LDOS of its spin- $\downarrow$  peak nor of its spin- $\uparrow$  peak vanishes at  $\mathbf{r}_{1,3}$  (or  $\mathbf{r}_2$ ), we find that at  $(JS)_{cr,3}$ , the order parameter at all three impurity sites decreases discontinuously. Moreover, when the LDOS of both the spin- $\downarrow$  and spin- $\uparrow$  peak vanishes at an impurity position, as is the case with  $\Psi_{odd}$  bound state at  $\mathbf{r}_2$  [see Figs. 11(d) and (e)], the superconducting order parameter at this impurity site is unaffected by the zero energy crossing of the bound state, as follows from Figs. 10(a) and (b). Thus the vanishing of the LDOS of only one of the spin- $\uparrow$  or spin- $\downarrow$  peaks at an impurity site can lead to a discontin-

uous increase in the superconducting order parameter at the phase transition, as discussed above.

## V. CONCLUSIONS

In conclusion, we have studied quantum interference phenomena in impurity structures consisting of two or three magnetic impurities located on the surface of an *s*-wave superconductor. By using a self-consistent BdG formalism<sup>21</sup>, we simultaneously investigated how quantum interference affects (a) the formation of impurity bound states in the LDOS, and (b) the spatial form of the superconducting order parameter.

We obtained three important results. First, we find that the characteristic signatures of quantum interference in the LDOS and in the superconducting order parameter are coupled. In particular, the larger the splitting between the hybridized bound states in the LDOS, the stronger is the suppression of the superconducting order parameter at the impurity sites. As a result, both the frequency of the bound states as well as the on-site order parameter exhibit Friedel-like oscillations as the distance between impurities is changed. Second, the suppression of the superconducting order parameter around impurities does not qualitatively change the signatures of quantum interference in the LDOS, thus demonstrating the robustness of quantum interference phenomena. The physical origin of this robustness lies in the fact that, while the superconducting order parameter is suppressed by impurities, it recovers its bulk value over a length scale which is set by the Fermi wavelength,  $\lambda_F$ , and not by the superconducting coherence length, which is typically much larger than  $\lambda_F$ . Third, we show that quantum interference leads to multiple first order quantum phase transitions in the superconductor, which are accompanied by a change in the spin polarization of the superconductor's ground state. The superconductor can be tuned through these transitions by increasing the impurities'

scattering strength or by changing the interimpurity distance, the latter being the experimentally more relevant tuning. These quantum transitions exhibit several characteristic features that are qualitatively different from the ones of a phase transition associated with a single magnetic impurity. In particular, the superconducting order parameter does not necessarily decrease discontinuously or undergo a  $\pi$ -phase shift, and, in certain cases, can even be enhanced at the transition. The difference between the critical values of  $JS$  for which these multiple transitions occur is determined by the hybridization strength, and is thus directly linked to the splitting between the impurity bound state energies. The tuning of the superconductor's spin polarization by changing the interimpurity distance potentially possesses important applications in the field of spin electronics<sup>19</sup> and quantum information technology<sup>20</sup> as it might lead to the creation of new types of quantum qubits.

Finally, we note that the relative orientation of the impurities' magnetic moments is determined in general by the residual interactions between the impurities, whose consideration is beyond the scope of this study. In case where the dominant contribution to the inter-impurity interaction arises from an RKKY-type process, the interesting question arises to what extent the interaction is affected by the formation of the hybridized impurity states. This question will be addressed in some future work.

## VI. ACKNOWLEDGEMENT

We would like to thank J.C. Davis, A. Kapitulnik and A. Yazdani for stimulating discussions. D.K.M. acknowledges financial support by the Alexander von Humboldt Foundation, the National Science Foundation under Grant No. DMR-0513415 and the U.S. Department of Energy under Award No. DE-FG02-05ER46225.

- 
- <sup>1</sup> H.C. Manoharan, C.P. Lutz, and D.M. Eigler, *Nature* (London) **403**, 512 (2000).  
<sup>2</sup> D.J. Derro *et al.*, *Phys. Rev. Lett.* **88**, 097002 (2002).  
<sup>3</sup> C. Chicanne *et al.*, *Phys. Rev. Lett.* **88**, 097402 (2002).  
<sup>4</sup> A.W. Holleitner *et al.*, *Phys. Rev. Lett.* **87**, 256802 (2001).  
<sup>5</sup> K.-F. Braun and K.-H. Rieder, *Phys. Rev. Lett.* **88**, 096801 (2002).  
<sup>6</sup> O. Pietzsch *et al.*, *Phys. Rev. Lett.* **92**, 057202 (2004).  
<sup>7</sup> L. Gross *et al.*, *Phys. Rev. Lett.* **93**, 056103 (2004).  
<sup>8</sup> G.A. Fiete *et al.*, *Phys. Rev. Lett.* **86**, 2392 (2001); A.A. Aligia, *Phys. Rev. B* **64**, 121102 (2001); K. Hallberg, A.A. Correa, and C.A. Balseiro, *Phys. Rev. Lett.* **88**, 066802 (2002); D. Porras *et al.*, *Phys. Rev. B* **63**, 155406 (2001); O. Agam and A. Schiller, *Phys. Rev. Lett.* **86**, 484 (2001); Y. Shimada *et al.*, *Surf. Sci* **514**, 89 (2002); M. Weissmann and H. Bonadeo, *Physica E* **10**, 544 (2001); M. Schmid and A.P. Kampf, *Ann. Phys.* **12**, 463 (2003); *ibid.* *Ann.*

- Phys.* **14**, 556 (2005).  
<sup>9</sup> M.E. Flatte, and D.E. Reynolds, *Phys. Rev. B* **61**, 14810 (2000).  
<sup>10</sup> D.K. Morr and A.V. Balatsky, *Phys. Rev. Lett.* **90**, 067005 (2003).  
<sup>11</sup> D.K. Morr and N. Stavropoulos, *Phys. Rev. B* **67**, 020502(R) (2003).  
<sup>12</sup> D. K. Morr and N. A. Stavropoulos, *Phys. Rev. Lett.* **92**, 107006 (2004); N. A. Stavropoulos and D. K. Morr, *Phys. Rev. B* **71**, 140501(R) (2005).  
<sup>13</sup> D.K. Morr and N. Stavropoulos, *Phys. Rev. B* **66**, 140508(R) (2002); L.Y. Zhu *et al.*, *Phys. Rev. B* **67**, 094508 (2003); B.M. Andersen and P. Hedegard, *Phys. Rev. B* **67**, 172505 (2003); C.H. Choi, *J. Kor. Phys. Soc.* **44**, 355 (2004).  
<sup>14</sup> N. A. Stavropoulos and D. K. Morr, preprint, cond-mat/0508059.

- <sup>15</sup> M.I. Salkola, A.V. Balatsky, J.R. Schrieffer, Phys. Rev. B **55**, 12648 (1997).
- <sup>16</sup> A. V. Balatsky, I. Vekhter, Jian-Xin Zhu, preprint, cond-mat/0411318.
- <sup>17</sup> A. Sakurai, Prog. Theor. Phys. **44**, 1472 (1970).
- <sup>18</sup> Y.B. Bazaliy and B.A. Jones, J. Appl. Phys. **87**, 5561 (2000).
- <sup>19</sup> S.A. Wolf *et al.*, Science **294**, 1488 (2001), and references therein.
- <sup>20</sup> B.E. Kane, Nature (London) **393**, 133 (1998).
- <sup>21</sup> P.G. de Gennes, *Superconductivity of Metals and Alloys* (Addison-Wesley, New York, 1989).
- <sup>22</sup> Th. Proslier *et al.*, preprint, cond-mat/0602023; O. Naaman, W. Teizer, and R. C. Dynes, Phys. Rev. Lett. **87**, 097004 (2001); J. Rodrigo, H. Suderow, and S. Vieira, Eur. Phys. Jour. B **40**, 483 (2004); S. H. Pan, E. W. Hudson, and J. C. Davis, Appl. Phys. Lett. **73**, 2992 (1998).
- <sup>23</sup> K. Satori *et al.*, J. Phys. Soc. Jpn. **61**, 3239 (1992).
- <sup>24</sup> A. Yazdani *et al.*, Science **275**, 1767 (1997).
- <sup>25</sup> Y. Lu, Acta Physics Sinica **21**, 75 (1965); H. Shiba, Prog. Theoret. Phys. **40**, 435 (1968).
- <sup>26</sup> However, for two magnetic impurities with  $\alpha = \pi$ , no hybridization of the impurity bound states takes place<sup>11</sup>.
- <sup>27</sup> P. Schlottmann, Phys. Rev. B **13**, 1 (1976).
- <sup>28</sup> A.I. Rusinov, JETP Lett. **9**, 85 (1969).
- <sup>29</sup> We find that for the 3-impurity system considered in Fig. 8 and a lattice with  $N_x = 28$  and  $N_y = 18$ , the bound state peaks highest in energy are too close to the superconducting coherence peaks to be properly resolved for  $JS < (JS)_{cr,1}$ . Therefore, we considered a slightly larger lattice with  $N_x = 34$  and  $N_y = 22$  for  $JS < (JS)_{cr,1}$  [see Fig. 8(a)] for which all three sets of bound state peaks are clearly resolved.